Hybrid Crosslinked Methylcellulose Hydrogel: A Predictable and Tunable Platform for Local Drug Delivery

*Malgosia M. Pakulska, Katarina Vulic, Roger Y. Tam, and Molly S. Shoichet**

Hydrogels are a ubiquitous tool in the field of regenerative medicine for both drug and cell delivery.[1] Researchers have created hydrogels that are biocompatible, injectable, in situ gelling, minimally swelling, biodegradable, or long-lasting; however, engineering a hydrogel to have many of these properties often comes at the expense of others.

Both chemically and physically crosslinked hydrogels have been used in regenerative medicine applications. Chemically crosslinked gels have the advantage of being longer lasting, yet require fine-tuning of the chemistry in order to be injectable, as covalent bonds must form in situ fast enough to avoid dilution and/or dispersion, yet slow enough to allow injection and minimal heat generation. The chemistry must also be aqueous-based and avoid cytotoxic crosslinkers and byproducts.[2] Physically crosslinked gels have the advantage of being responsive to environmental stimuli such as temperature or pH, but the noncovalent crosslinks are in dynamic equilibrium, resulting in faster resorption/erosion after injection. Higher polymer concentrations are often used to improve stability, but this can lead to increased osmotic pressure gradients and swelling which may cause tissue damage in a confined space.

Combining both chemical and physical crosslinks in a single hydrogel has emerged as a promising way to obtain hydrogels with improved biostability while maintaining injectability. Hydrogels combining the thermogelling properties of methacrylated poly(*N*-isopropylacrylamide) (p-NIPAAM) and chemical crosslinking with thiolated hyaluronan (HA) or poly(ethylene glycol) (PEG) have been studied.[3,4] Similarly, p-NIPAAM has been modified with epoxy rings for chemical crosslinking with a diamine crosslinker.[5] Thiol-acrylate chemical crosslinking has also been combined with the physical gelation of thiol modified chitosan (Ch-SH) and β-glycerophosphate.[6] However, all these gels are mixed just prior to use to retain injectability and have the chemical crosslinking occurring in situ, requiring fine-tuned, aqueous-based reactions that proceed at an optimal rate and use no cytotoxic reagents. Other examples of hydrogels with both physical and chemical crosslinking use UV-activated photocrosslinkers for in situ gelation.[7] This restricts the site of injection to regions in close proximity to the surface of the body and necessitates the use of UV irradiation, which may have deleterious effects.[8] Additionally, while these hydrogels are interesting and promising, previous reports are limited to the study of only one formulation, thereby restricting the depth of understanding of the formulation and its effect on gel properties.

Using design of experiment (DOE), we engineered a physically and chemically crosslinked hybrid hydrogel based on methylcellulose (MC) (**Figure 1**a). To gain insight into utility and usability, we tested the gel formulation in vitro for protein release and in vivo for biocompatibility. Notably, in this formulation, the chemical crosslinking is complete prior to use, yet the gel remains injectable allowing for easy storage, facile timing of injection, and no further manipulation after injection in vivo.

As an inverse thermogelling polymer, MC naturally forms physical crosslinks, yet typically requires high temperatures or long times for these crosslinks to form.[9] When modified with thiol groups, MC-thiol can be crosslinked with poly(ethylene glycol)-bismaleimide, PEG-MI_2, resulting in a Michael-type addition and a chemically crosslinked hydrogel. This reaction occurs within minutes at physiological pH and room temperature and requires no toxic catalysts (Figure S2, Supporting Information).[10]

Using a design of experiment (DOE) approach, we develop empirical equations that allow prediction and tuning of the hydrogel mechanical and swelling properties based on three variables: MC content, thiol content, and maleimide to thiol ratio. DOE is a powerful method as it allows us to study strategically chosen points while still obtaining an accurate representation of the entire response surface within this range of points. Although DOE has been used in engineering process design for decades, its utility for the study of hydrogel synthesis is more recent.[11,12]

With this knowledge, we are able to create a hybrid hydrogel, XMC, that is injectable, in situ gelling, minimally swelling, and long-lasting. With $G' > G''$ as the accepted rheological definition of a gel, XMC is a gel before injection whereas a physically crosslinked MC gel with the same weight percent polymer takes 10 min to form a gel at 37 °C (Figure 1b). XMC also swells less than the physically crosslinked MC gel or physically crosslinked MC gel with added PEG-MI_2, stabilizing after only 6 h. Additionally, the physically crosslinked MC gel with or without added PEG-MI_2 shows substantial mass loss over 35 d while XMC does not (Figure 1c). Importantly, the

M. M. Pakulska, Dr. R. Y. Tam, Prof. M. S. Shoichet
Department of Chemical Engineering
and Applied Chemistry
University of Toronto
200 College St., Toronto, ON M5S 3E5, Canada
E-mail: molly.shoichet@utoronto.ca
M. M. Pakulska, Dr. R. Y. Tam, Prof. M. S. Shoichet
Institute for Biomaterials and Bioengineering
University of Toronto
164 College St., Rm 407, Toronto, ON M5S 3G9, Canada
Dr. K. Vulic, Prof. M. S. Shoichet
Department of Chemistry
University of Toronto
80 St. George St., Toronto, ON M5S 3H6, Canada

DOI: 10.1002/adma.201502767

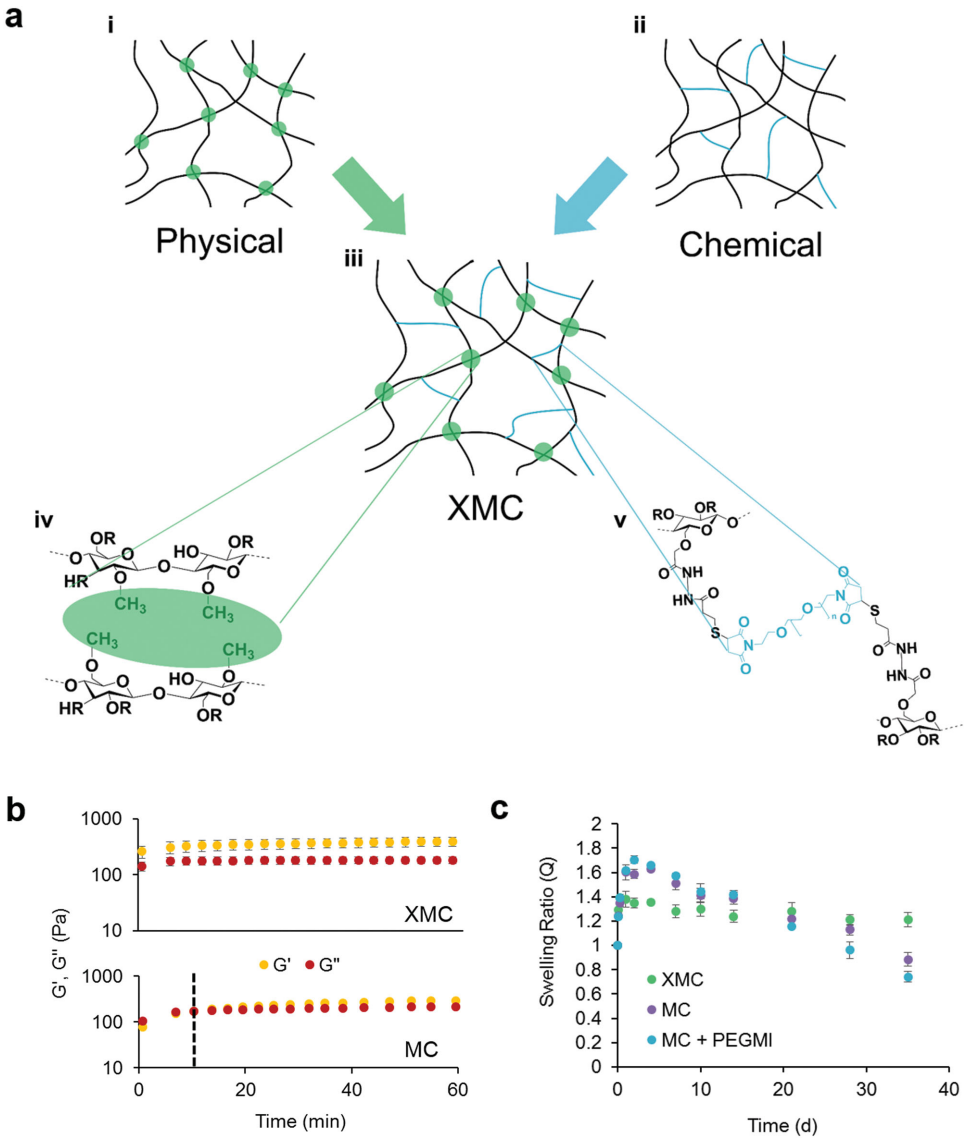

Figure 1. a) Schematic diagram of a (i) physically and (ii) chemically crosslinked hydrogel. (iii) Our crosslinked methylcellulose (XMC) is a hybrid hydrogel that is both physically and chemically crosslinked. (iv) The physical crosslinks consist of hydrophobic interactions between the methylcellulose chains while (v) the chemical crosslinks are formed by reaction of a thiol-modified MC with a PEG-bismaleimide crosslinker. b) Shear storage and loss moduli (G', G'') for XMC and MC hydrogels. Top panel: XMC hydrogel (5 wt% MC, 0.1 μmol thiol/100 μL, 0.75:1 ratio maleimide–thiol, $n = 5$) over time at 37 °C after 10 min of equilibration at 4 °C. Bottom panel: MC hydrogel (5 wt% MC) over time at 37 °C after 10 min of equilibration at 4 °C. Dotted line marks the gelation point ($G' > G''$). c) Swelling ratio of the XMC hydrogel, MC hydrogel, and MC hydrogel with added PEG-MI_2 over time at 37 °C ($n = 3$). This also indirectly depicts stability of the hydrogel over a 35 d period (mean ± standard deviation plotted).

chemical crosslinking reaction is complete prior to injection of XMC (Figure S2, Supporting Information), providing improved control over gelation and avoiding side reactions within the tissue. The chemical and physical crosslinks are balanced in such a way that the hydrogel is still injectable after chemical crosslinking is complete, with the physical crosslinks strengthening upon exposure to 37 °C due to the inverse thermogelling properties of MC. After injection, the hydrogel requires no further manipulation and remains localized at the injection site.

We further demonstrate the practical application of this hybrid XMC hydrogel for drug delivery to the injured rat spinal cord. An injectable, localized drug delivery system is especially compelling for treatment of central nervous system (CNS) diseases and injuries because the presence of the blood spinal cord barrier (BSCB) or the blood brain barrier (BBB) prevents the delivery of most systemically administered therapeutics. In particular, spinal cord injury (SCI) can benefit from such an injectable, long-lasting drug delivery system, as the current catheter minipump systems for sustained drug treatment are prone to complications and infection[13] and cerebrospinal fluid flow creates a challenging environment for in situ gelation and local delivery.

We use a face-centered central composite design with center points (**Figure 2**a) to avoid a trial-and-error approach and

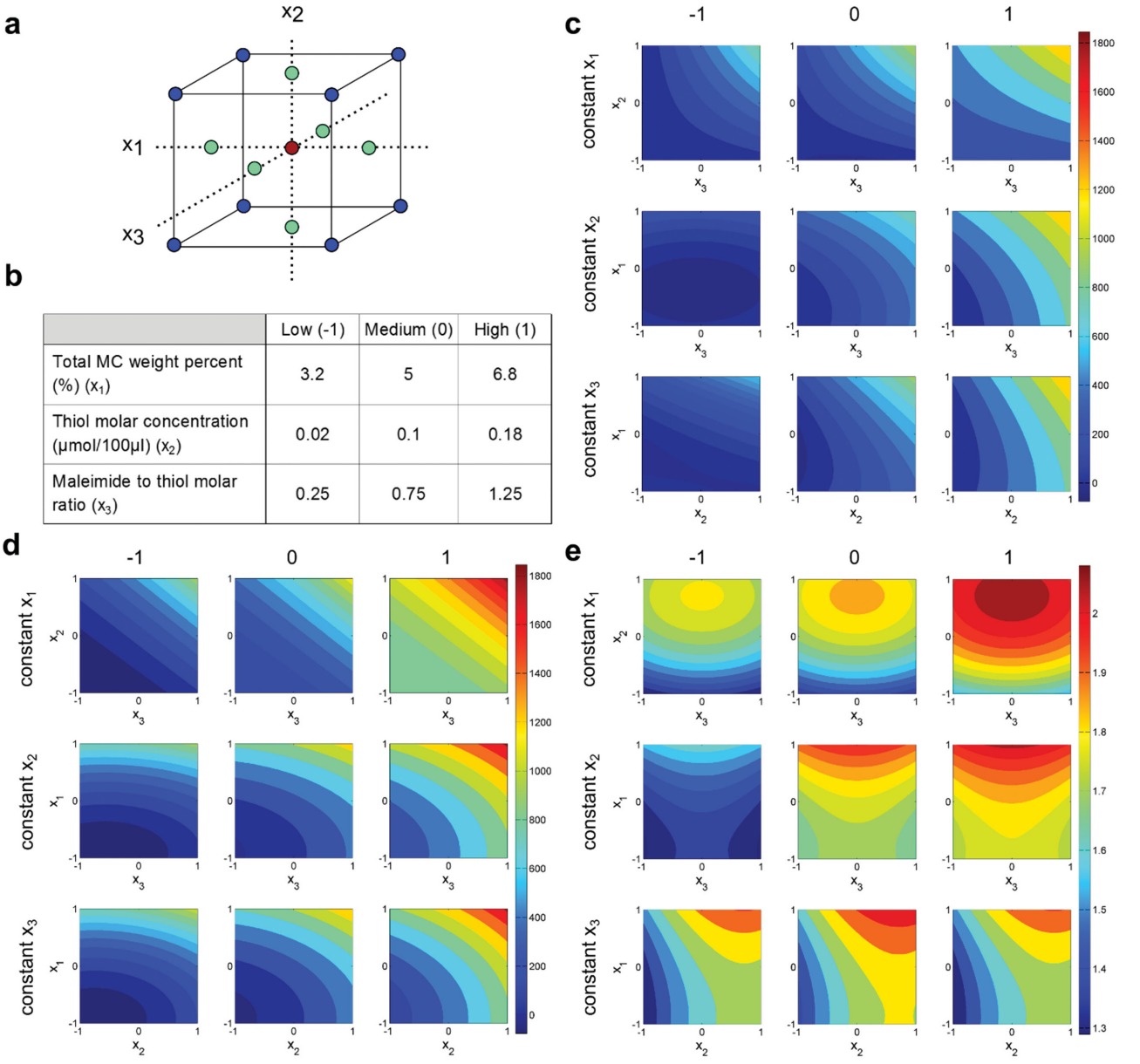

	Low (-1)	Medium (0)	High (1)
Total MC weight percent (%) (x_1)	3.2	5	6.8
Thiol molar concentration (μmol/100μl) (x_2)	0.02	0.1	0.18
Maleimide to thiol molar ratio (x_3)	0.25	0.75	1.25

Figure 2. a) Design space showing the points used in the face-centered central composite design with center points. b) Table showing the ranges of each of the three independent variables. Variables were normalized for analysis such that the values fell between −1 and 1. The value at 0 is the center point. c–e) Contour plots showing the effect of MC weight percent (x_1), moles of thiol (x_2), and ratio of maleimide to thiol (x_3) on: c) initial shear storage modulus (G') at 37 °C, d) G' after 1 h at 37 °C, and e) maximum swelling at 37 °C of XMC hydrogels. In each plot, one of x_1, x_2, or x_3 is held constant at a low (−1), medium (0), or high (1) value and the effect of varying the other two variables between −1 and 1 on each outcome measure is plotted.

thoroughly investigate the effect of each of three independent variables on the properties of the hydrogel. We control the total MC weight percent (x_1), the total moles of thiol (x_2) within the hydrogel, and the ratio of crosslinker (PEG-MI_2) to thiol (x_3). Variables are normalized for analysis such that the lowest value is −1 and the highest value is +1. Figure 2b shows the ranges used for each variable. Each gel was evaluated in terms of initial shear storage modulus (G') upon injection to 37 °C (Y_1), shear storage modulus after 1 h at 37 °C (Y_2), and maximum swelling after incubation at 37 °C (Y_3). Individual gel data are summarized in Table S1 and Figures S3 and S4 (Supporting Information). Although G' of the gels has not reached a plateau after 1 h, longer rheology studies show that the majority of the differences between gels are seen within the first hour and trends do not change even after 5 h (Figure S5, Supporting Information). The data are fit to a ten-parameter second-order model in three factors and ANOVA with an F test is used to eliminate effects that are not significant at a 95% level of confidence. This allowed us to generate models that relate the three independent variables with the three outcome measures.

$$Y_1 = 121.2x_1^2 + 9.75x_2^2 + 29.8x_3^2 + 189.3x_1 + 286.1x_2 + 212.8x_3 + 98.3x_1x_2 + 207.9x_2x_3 + 255.5 \quad (1)$$

$$Y_2 = 237.6x_1^2 + 88.1x_2^2 + 65.2x_3^2 + 437.0x_1 + 287.2x_2 + 229.6x_3 + 155.3x_2x_3 + 345.8 \quad (2)$$

$$Y_3 = 0.0790x_1^2 - 0.151x_2^2 - 0.0752x_3^2 + 0.135x_1 + 0.216x_2 + 1.79 \quad (3)$$

The adjusted R^2 values for Y_1, Y_2, and Y_3 are 0.985, 0.992, and 0.993, respectively. Model adequacy was validated using residual plots and normal probability plots (Figure S6, Supporting Information). A visual representation of these equations was made using contour plots (Figure 2c–e). These plots show the effect of varying two of the three independent variables on an outcome measure while the third independent variable remains constant at a low (−1), medium (0), or high (1) value.

Initial G' depends on all three of the independent variables relatively equally (Figure 2c). This represents a balance between the intrinsic interactions between MC chains in solution and the interactions promoted by the thiol-maleimide crosslinks. When either the amount of thiol or the maleimide:thiol ratio is held at a low value, initial G' is almost solely dependent on MC concentration because crosslinking density is very low; however, when increased to medium or high values, crosslinking begins to appreciably decrease the average molecular weight of the polymer between crosslinks (M_c) and influences G' significantly,[14,15] as has also been observed by others.[16,17]

The value of G' after 1 h at 37 °C depends most strongly on the MC content, which is not surprising since MC is the thermogelling element (Figure 2d). For a constant thiol content and maleimide:thiol ratio, the magnitude of the final G' increases proportionally to the square of MC content. According to Clark and Ross–Murphy this would be indicative of the limiting case when the polymer concentration is much greater than the critical concentration C_0 required to form a network.[18] Higher MC content may also promote chain entanglement, which has been shown to increase polymer strength more than would be expected from classic intermolecular interactions.[19,20] Thiol content and maleimide–thiol ratio have the greatest effect on final G' when they are at their highest value or when MC content is low. As with initial G', this is likely because only then is the crosslinking density high enough to appreciably decrease M_c.

Interestingly, neither the initial G' nor the final G' values are highest at a 1:1 ratio of malemide:thiol. This has been observed by others[21,22] and is likely because the reaction is not 100% efficient, as the diffusion of the crosslinker chains is likely reduced with increasing gel viscosity.

In contrast to the modulus, the maximal gel swelling does not reveal any significant interaction effects between the variables. Hydrogels swell until the increase of elastic energy of the stretching polymer chains equals the decrease in the free energy of polymer and solvent mixing.[23,24] Increasing the total percentage of MC while holding the thiol content and maleimide:thiol ratio constant effectively increases M_c and therefore decreases the rate at which the free energy of stretching increases (Figure 2e). This allows for increased solvent uptake (resulting in increased swelling) before the rate of increase in free energy of stretching becomes equal to the rate of decrease in free energy of mixing.

Both the crosslinker ratio and thiol content have a more complex, somewhat surprising relationship with swelling. One might expect that any increase in thiol content or crosslinker ratio would decrease swelling due to the increased crosslink density (and decreased M_c). However, for both thiol content and crosslinker ratio, there is an initial increase in swelling up to a certain threshold value, followed by a decrease. The initial increase is likely due to an enhanced osmotic driving force because of changes in molecular composition. PEG is extremely hygroscopic and increasing the crosslinker concentration (and thus the PEG concentration) would promote water uptake.[25] It could also be due to additional driving forces such as the introduction of ionizable groups in the form of thiols and hydrazides.[26,27] There is a threshold thiol content and maleimide:thiol ratio above which the crosslinking density becomes so high that the unfavorable stretching of the crosslinked polymer dominates any osmotic driving forces and the maximum swelling decreases again. It is these nonintuitive results that reinforce the necessity of this type of analysis. By picking only one or two points within the design space, one may miss key insights into optimal hydrogel design strategies.

The majority of these formulations are defined rheologically as gels after crosslinking ($G' > G''$); however, those with the lowest amount of thiol (0.02 µmol thiol/100 µL gel) were not. For these, we were able to measure the time to gelation upon temperature increase from 4 to 37 °C (Table S2, Supporting Information). In general, the time to gelation decreases with increasing MC content as expected,[28] except for gel 5 where the modulus is still very low (Figure S3, Supporting Information).

For minimally invasive surgery, injection through a fine needle is required and thus we investigated which gels were injectable through a 30 gauge needle in vitro (Table S2, Supporting Information). Of all the gels tested, only the three gels with the highest MC content of 6.8 wt% were not injectable. In order to flow through a fine needle, the stress applied during injection needs to exceed the yield strength of the material. In such high weight percent gels, increased interchain interactions, including entanglements, likely prevent this.[19] Given that the rheological properties of the same gel before and after injection through a 30-gauge needle are largely the same, the network structure of the gel is maintained after injection (Figure S7, Supporting Information).

In order to control drug release from the hydrogel, we investigated: (1) combining XMC with drug-loaded poly(lactic-*co*-glycolic acid) (PLGA) nanoparticles (np) and (2) modifying some of the MC chains for affinity-based drug release. PLGA nano- or microparticles have been used extensively for controlled release of small molecule and protein drugs.[29,30] Release is governed by diffusion through water-filled channels coupled with bulk polymer degradation.[31] Combining PLGA particles with a hydrogel allows particle localization, decreases initial burst, and further prolongs release.[32–35] Although some studies have shown that PLGA np act to strengthen hydrogels,[34,36] combining up to 10 wt% PLGA nanoparticles into our XMC hydrogel did not affect its rheological properties, likely because

ADVANCED MATERIALS
www.advmat.de

www.MaterialsViews.com

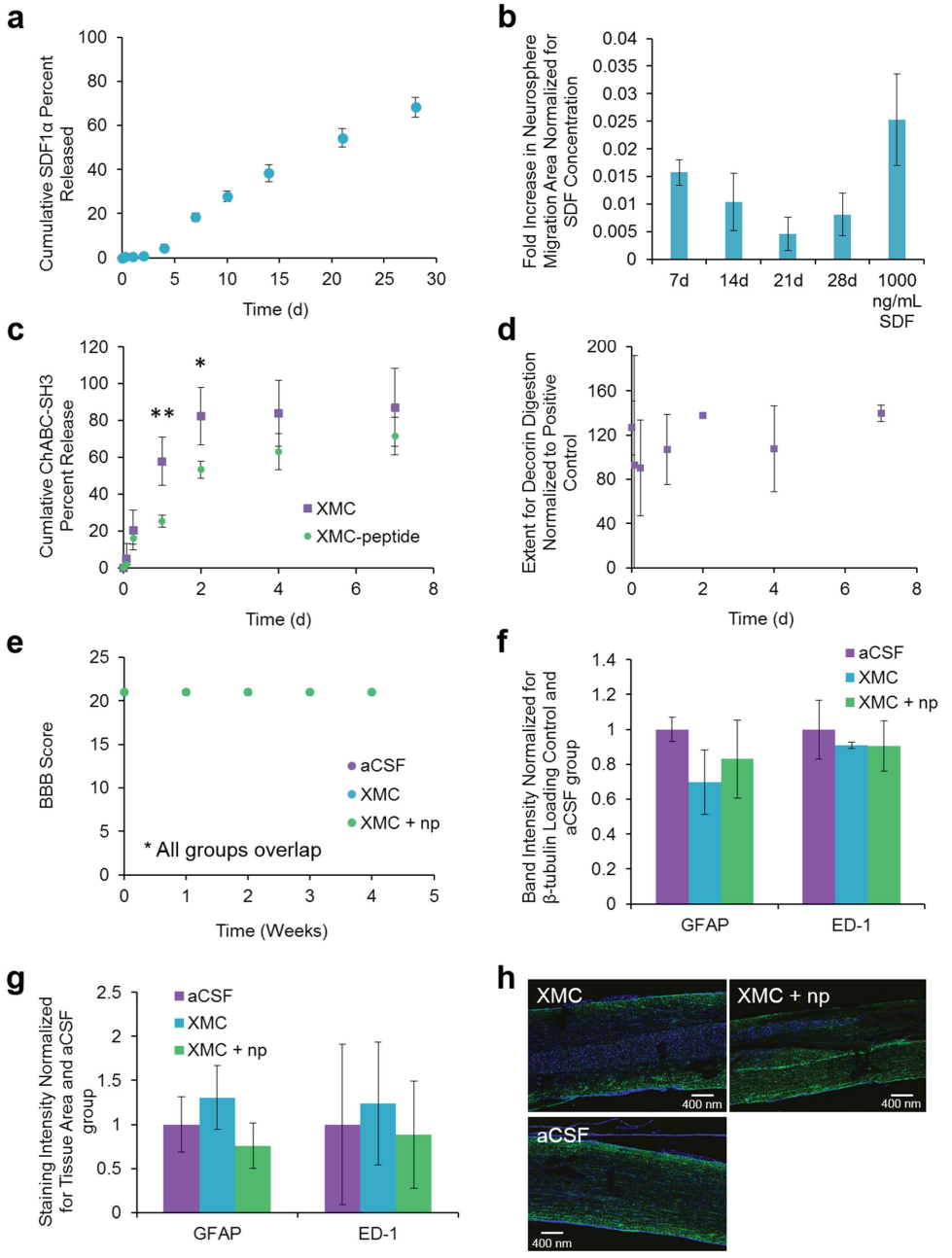

Figure 3. a) In vitro release profile of SDF1α encapsulated in PLGA nanoparticles (np) embedded within the XMC hydrogel (5 wt% MC, 0.1 µmol thiol/100 µL, 0.75:1 ratio maleimide:thiol, $n = 3$ independent gels, mean ± cumulative sd plotted). b) SDF released from PLGA np embedded in XMC promotes migration of adult rat spinal cord NSPCs from neurospheres plated on fibronectin. The SDF concentration in each sample was measured by ELISA and each sample was diluted to a final concentration of 1000 ng mL^{-1} SDF (7 d, 14 d) or to the maximum available concentration (21 d, 28 d). Migration areas were normalized to a 0 ng mL^{-1} SDF control performed on the same day and the measured SDF concentration. $n = 3$ independent releases (two wells per release, four neurospheres quantified per well), mean ± sd plotted. All values are significantly different from 0 at a 95% level of confidence ($p < 0.05$). c) In vitro affinity-based release of ChABC-SH3 from an XMC hydrogel where some of the MC was modified with SH3 binding peptides (XMC-peptide) or from unmodified XMC. Release from unmodified XMC is significantly faster than release from XMC-peptide by two-way ANOVA ($p < 0.001$). Stars indicate significant difference between cumulative percent released at 1 ($p < 0.01$) and 2 d ($p < 0.05$). d) Activity of released ChABC-SH3 measured using a DMMB assay for decorin degradation ($n = 3$ independent gels, mean ± cumulative sd plotted). e) BBB open-field locomotor scores of all animals. A score of 21 represents no motor deficit.[57] f) Quantitation of western blots from tissue revealed no significant increase in GFAP (activated astrocytes) or ED-1 (activated macrophages/microglia) expression 28 d after intrathecal injection of XMC or XMC with PLGA np compared to intrathecal injection of artificial cerebrospinal fluid (aCSF). Band intensity was quantified using ImageJ software. $n = 3$ animals per group, mean ± sd plotted. g) Quantitation of spinal cord tissue staining 28 d after injection of XMC with or without PLGA np into the intrathecal space of healthy rats. Neither gel formulation showed upregulation of GFAP or ED-1 compared to injection of aCSF ($n = 3$ animals per group, mean ± sd plotted). h) Representative parasagittal sections of spinal cord from each of the treatment groups. Green = GFAP, red = ED-1, blue = DAPI.

the effect is masked by the strengthening of the gel due to chemical crosslinking (Figure S8, Supporting Information). Here, we encapsulated stromal cell derived factor 1α (SDF1α) in PLGA np. SDF1α is a chemokine that is upregulated after central nervous system injury[37,38] and may be involved in the homing of neural stem progenitor cells (NSPCs) to the injury site.[39–41] We followed the release of SDF1α from the np embedded in our XMC hydrogel. We obtained sustained, zero-order release of SDF1α from our system for a period of 28 d (**Figure 3**a). The harsh solvents and conditions involved in PLGA np formulation can often be detrimental to protein therapeutics;[42–44] importantly, some of the SDF1α released from our system remained bioactive for the entire release period as measured by its ability to increase adult rat spinal cord NSPC migration in vitro (Figure 3b).

Affinity-based release relies on either the inherent or engineered affinity between the protein therapeutic and scaffold from which it is being released. The reversible interaction between these two binding partners results in sustained release. Affinity release is a great alternative for protein therapeutics that are too fragile for conventional encapsulation procedures, such as chondroitinase ABC (ChABC), a bacterial enzyme that has been used extensively to degrade inhibitory molecules in the glial scar after spinal cord injury.[45,46] XMC was modified for affinity-based release by incorporating MC that had been covalently linked to a Src homology domain 3 (SH3) binding peptide, as previously described.[46,47] This allowed sustained release of a ChABC-SH3 fusion protein from XMC for a period of 7 d while maintaining its activity, compared to only 2 d in an unmodified XMC gel (Figure 3c). The addition of peptide modified MC and ChABC-SH3 to the XMC hydrogel did not substantially affect its rheological properties (Figure S9, Supporting Information).

Complete, 100% release is rarely seen in protein release studies and this was also the case here. This could be due to the protein denaturing and aggregating over time within the gel, in the release media, or during freezing of the release samples before measurement.[48,49]

We tested the biocompatibility of XMC in the cerebrospinal fluid filled intrathecal space that surrounds the rat spinal cord. In vivo tests were performed with the center point gel (5 wt% MC, 0.1 µmol thiol/100 µL, 0.75:1 maleimide:thiol ratio) as it was injectable after crosslinking (Table S2, Supporting Information) and had rheological properties and a swelling ratio previously shown to be safe for intrathecal injection[34,50,51] (Figure 3d,e). Injection of a hydrogel in a confined space can be deleterious, causing tissue compression. Importantly, this XMC hydrogel was safe after intrathecal injection. No behavioural deficits were observed in weekly locomotor scoring of the animals (Figure 3f). We also observed no increase in activated astrocytes (GFAP staining) or activated microglia/macrophages (ED-1 staining) at 28 d after injection by western blot (Figure 3g) or immunohistochemistry (Figure 3h,i) compared to intrathecal injection of artificial cerebrospinal fluid (aCSF). These data indicate that the XMC hydrogel is safe and biocompatible.

Despite the lack of biodegradable bonds within the XMC, we did not observe any remaining material on the spinal cords after 4 weeks in vivo by visual inspection or after 8 weeks in vivo by polarized light microscopy[52] (data not shown). A similar erosion and elimination of noncrosslinked high molecular weight MC has previously been observed in the intrathecal space of rats.[53] The gel likely erodes as the polymer chains disentangle[54] and dissolves due to fluid flow within the intrathecal space. Smaller polymer chains may enter the bloodstream and be eliminated via the kidneys while larger chains may extravasate into the tissue.[55,56] This hybrid hydrogel is therefore safe to use in rat models of spinal cord injury and is able to control the release of two molecules relevant to spinal cord regeneration either via affinity release or np encapsulation.

Using a face-centered central composite design with center points, we elucidated key relationships between the gel composition and properties, allowing us to design hydrogels with varying mechanical strength and swelling for a given function. This methodology is broadly applicable and demonstrated herein with XMC, a hybrid hydrogel containing both physical and chemical crosslinks. Independent control over chemical and physical crosslink density allows the formation of an XMC gel that is injectable yet long-lasting. Moreover, we have demonstrated the utility of XMC for use in minimally invasive surgeries and sustained biomolecule release.

Supporting Information

Supporting Information is available from the Wiley Online Library or from the author.

Acknowledgements

The authors thank Peter Poon for performing all surgeries, Dr. Andrea Mothe for the rat spinal cord NSPCs, and Dr. Charles H. Tator for helpful advice and discussion. The authors are grateful to NSERC and CIHR for funding and to the NSERC Vanier scholarship (to M.P.).
Note: In the top part of panel b of Figure 1, the G′ and G″ curves appeared mislabeled on initial publication online. This was corrected here on September 4, 2015.

Received: June 9, 2015
Published online: July 16, 2015

[1] N. Annabi, A. Tamayol, J. A. Uquillas, M. Akbari, L. E. Bertassoni, C. Cha, G. Camci-Unal, M. R. Dokmeci, N. A. Peppas, A. Khademhosseini, *Adv. Mater.* **2014**, *26*, 85.
[2] M. Patenaude, N. M. B. Smeets, T. Hoare, *Macromol. Rapid Commun.* **2014**, *35*, 598.
[3] K. W. M. Boere, B. G.Soliman, D. T. S. Rijkers, W. E. Hennink, T. Vermonden, *Macromolecules* **2014**, *47*, 2430.
[4] R. Censi, P. J. Fieten, P. di Martino, W. E. Hennink, T. Vermonden, *Macromolecules* **2010**, *43*, 5771.
[5] T. N. Vo, A. K. Ekenseair, F. K. Kasper, A. G. Mikos, *Biomacromolecules* **2013**, *15*, 132.
[6] C. Chen, L. Wang, L. Deng, R. Hu, A. Dong, *J. Biomed. Mater. Res. A* **2013**, *101*, 684.
[7] H. D. Lu, D. E. Soranno, C. B. Rodell, I. L. Kim, J. A. Burdick, *Adv. Healthc. Mater.* **2013**, *2*, 1028.
[8] N. E. Fedorovich, M. H. Oudshoorn, D. van Geemen, W. E. Hennink, J. Alblas, W. J. A. Dhert, *Biomaterials* **2009**, *30*, 344.
[9] L. Li, P. M. Thangamathesvaran, C. Y. Yue, K. C. Tam, X. Hu, Y. C. Lam, *Langmuir* **2001**, *17*, 8062.

[10] C. M. Nimmo, M. S. Shoichet, *Bioconjug. Chem.* **2011**, *22*, 2199.
[11] H. Omidian, K. Park, *J. Bioactive Compatible Polym.* **2002**, *17*, 433.
[12] F. H. A. Rodrigues, A. G. B. Pereira, A. R. Fajardo, E. C. Muniz, *J. Appl. Polym. Sci.* **2013**, *128*, 3480.
[13] K. H. Knight, F. M. Brand, A. S. McHaourab, G. Veneziano, *Croatian Med. J.* **2007**, *48*, 22.
[14] L. E. Nielsen, *J. Macromol. Sci.Part C* **1969**, *3*, 69.
[15] K. S. Anseth, C. N. Bowman, L. Brannon-Peppas, *Biomaterials* **1996**, *17*, 1647.
[16] K. Y. Lee, J. A. Rowley, P. Eiselt, E. M. Moy, K. H. Bouhadir, D. J. Mooney, *Macromolecules* **2000**, *33*, 4291.
[17] J. P. Best, J. Cui, M. Müllner, F. Caruso, *Langmuir* **2013**, *29*, 9824.
[18] A. H. Clark, S. B. Ross-Murphy, *Br. Polym. J.* **1985**, *17*, 164.
[19] W. Graessley, in *The Entanglement Concept in Polymer Rheology*, Springer, Berlin, Heidelberg **1974**, pp. 1–179.
[20] G. Heinrich, T. A. Vilgis, *Macromolecules* **1993**, *26*, 1109.
[21] N. Paradee, A. Sirivat, S. Niamlang, W. Prissanaroon-Ouajai, *J. Mater. Sci. Mater. Med.* **2012**, *23*, 999.
[22] M. P. Lutolf, J. A. Hubbell, *Biomacromolecules* **2003**, *4*, 713.
[23] N. A. Peppas, E. W. Merrill, *J. Appl. Polym. Sci.* **1977**, *21*, 1763.
[24] J. C. Bray, E. W. Merrill, *J. Appl. Polym. Sci.* **1973**, *17*, 3779.
[25] J. A. Baird, R. Olayo-Valles, C. Rinaldi, L. S. Taylor, *J. Pharm. Sci.* **2010**, *99*, 154.
[26] F. Ganji, S. Vasheghani-Farahani, E. Vasheghani-Farahani, *Iranian Polym. J.* **2010**, *19*, 375.
[27] R. Marcombe, S. Q. Cai, W. Hong, X. H. Zhao, Y. Lapusta, Z. G. Suo, *Soft Matter* **2010**, *6*, 784.
[28] N. Sarkar, *Carbohydrate Polym.* **1995**, *26*, 195.
[29] F. Danhier, E. Ansorena, J. M. Silva, R. Coco, A. Le Breton, V. Preat, *J. Controlled Release* **2012**, *161*, 505.
[30] I. Bala, S. Hariharan, M. N. Kumar, *Crit. Rev. Ther. Drug Carrier Syst.* **2004**, *21*, 387.
[31] L. K. Chiu, W. J. Chiu, Y. L. Cheng, *Int. J. Pharm.* **1995**, *126*, 169.
[32] H. Geng, H. Song, J. Qi, D. Cui, *Nanoscale Res. Lett.* **2011**, *6*, 312.
[33] J. C. Stanwick, M. D. Baumann, M. S. Shoichet, *J. Controlled Release* **2012**, *160*, 666.
[34] M. D. Baumann, C. E. Kang, J. C. Stanwick, Y. Wang, H. Kim, Y. Lapitsky, M. S. Shoichet, *J. Controlled Release* **2009**, *138*, 205.
[35] D.-H. Kim, D. C. Martin, *Biomaterials* **2006**, *27*, 3031.
[36] E. A. Appel, M. W. Tibbitt, M. J. Webber, B. A. Mattix, O. Veiseh, R. Langer, *Nat. Commun.* **2015**, *6*, 6295.
[37] W. D. Hill, D. Hess, A. Martin-Studdard, J. J. Carothers, J. Zheng, D. Hale, M. Maeda, S. C. Fagan, J. E. Carroll, S. J. Conway, *J. Neuropathol. Exp. Neurol.* **2004**, *63*, 84.
[38] H. Takeuchi, A. Natsume, T. Wakabayashi, C. Aoshima, S. Shimato, M. Ito, J. Ishii, Y. Maeda, M. Hara, S. U. Kim, J. Yoshida, *Neurosci. Lett.* **2007**, *426*, 69.
[39] J. Imitola, K. Raddassi, K. I. Park, F. J. Mueller, M. Nieto, Y. D. Teng, D. Frenkel, J. Li, R. L. Sidman, C. A. Walsh, E. Y. Snyder, S. J. Khoury, *Proc. Natl. Acad. Sci. USA* **2004**, *101*, 18117.
[40] H. Peng, Y. Huang, J. Rose, D. Erichsen, S. Herek, N. Fujii, H. Tamamura, J. Zheng, *J. Neurosci. Res.* **2004**, *76*, 35.
[41] V. M. Tysseling, D. Mithal, V. Sahni, D. Birch, H. Jung, A. Belmadani, R. J. Miller, J. A. Kessler, *J. Neuroinflammation* **2011**, *8*, 1742.
[42] M. van de Weert, W. E. Hennink, W. Jiskoot, *Pharmaceut. Res.* **2000**, *17*, 1159.
[43] C. Pérez, I. J. Castellanos, H. R. Costantino, W. Al-Azzam, K. Griebenow, *J. Pharm. Pharmacol.* **2002**, *54*, 301.
[44] A. Giteau, M. C. Venier-Julienne, A. Aubert-Pouëssel, J. P. Benoit, *Int. J. Pharm.* **2008**, *350*, 14.
[45] E. J. Bradbury, L. M. Carter, *Brain Res. Bull.* **2011**, *84*, 306.
[46] M. M. Pakulska, K. Vulic, M. S. Shoichet, *J. Controlled Release* **2013**, *171*, 11.
[47] K. Vulic, M. S. Shoichet, *J. Am. Chem. Soc.* **2011**, *134*, 882.
[48] E. Cao, Y. Chen, Z. Cui, P. R. Foster, *Biotechnol. Bioeng.* **2003**, *82*, 684.
[49] W. Wang, *Int. J. Pharm.* **1999**, *185*, 129.
[50] D. Gupta, C. H. Tator, M. S. Shoichet, *Biomaterials* **2006**, *27*, 2370.
[51] M. D. Baumann, C. E. Kang, C. H. Tator, M. S. Shoichet, *Biomaterials* **2010**, *31*, 7631.
[52] M. Parthasarathy, S. Sethuraman, in *Natural and Synthetic Biomedical Polymers* (Eds: S. Deng, G. Kumbar, T. Cato, M. Laurencin), Elsevier, Oxford **2014**, Ch. 2, pp. 33–42.
[53] C. E. Kang, P. C. Poon, C. H. Tator, M. S. Shoichet, *Tissue Eng. Part A* **2009**, *15*, 595.
[54] B. Narasimhan, N. A. Peppas, in *Polymer Analysis Polymer Physics*, Springer, Berlin **1997**, pp. 157–207.
[55] L. W. Seymour, R. Duncan, J. Strohalm, J. Kopecek, *J. Biomed. Mater. Res.* **1987**, *21*, 1341.
[56] E. Markovsky, H. Baabur-Cohen, A. Eldar-Boock, L. Omer, G. Tiram, S. Ferber, P. Ofek, D. Polyak, A. Scomparin, R. Satchi-Fainaro, *J. Controlled Release* **2012**, *161*, 446.
[57] D. M. Basso, M. S. Beattie, J. C. Bresnahan, *J. Neurotrauma* **2009**, *12*, 1.